

# An effective model-based thruster failure detection method for dynamically positioned ships

Tongtong Wang, Guoyuan Li, Robert Skulstad, Vilmar Æsøy and Houxiang Zhang

*Department of Ocean Operations and Civil Engineering*

*Norwegian University of Science and Technology*

*Postboks 1517, N-6025, Aalesund, Norway*

*{tongtong.wang, guoyuan.li, robert.skulstad, vilmar.aesoy, hozh}@ntnu.no*

**Abstract**—This paper presents an effective model-based thruster failure detection and isolation method for dynamically positioned (DP) offshore surface vessels. A DP vessel is supposed to maintain its position and heading at a reference point exclusively by means of thrusters. The occurrence of thruster failure may cause significant performance losses. Therefore, it is of great practical importance to timely detect and isolate thruster failures. In our proposed method, according to the prior knowledge of mathematical model of a DP ship, estimated model states can be obtained as reference. Wind disturbances, due to its great influence on the thruster diagnosis of the DP vessel, is taken into account. A new attitude based residual generator is designed. A failure can be identified once it exceeds a threshold. To further isolate the failure, a slide window concept together with a probability analysis is applied to the residual, until a concrete thrust failure is found. Simulation experiments of DP operation under different thruster failure cases are conducted in a professional simulator. The results show the proposed method is able to detect and isolate these thruster failures.

**Index Terms**—Thruster failure, failure detection and isolation, dynamic positioning, offshore surface vessel.

## I. INTRODUCTION

With the development and employment of advanced technologies such as digital twins [1] and cloud computing [2] on modern vessels, marine operation steps in the era of intelligence. In various maritime industrial sectors, digital twins are being used for monitoring, diagnostics and prognostics to optimize asset performance and utilization. During operation, the digital twin becomes a system for integration, processing, and analysis of the operational data. Ideally, the digital twin will provide behaviour predictions and life cycle service support for ship operators. Ship health management, as an essential part of our ongoing project "digital twins for vessel life cycle service", should be aware of the changing operating regimes during maritime operations to optimize asset performance. In the marine operation phase, the dynamic positioning is an important maneuver that acts to maintain a vessel's position and heading at a reference point by means of exclusively activating its thrusters [3] [4]. In practice, thrusters inevitably undergo faults due to long-time operation in the complex ocean environment, which will cause the DP control system unstable, thereby reducing DP performance. Therefore, it is of great significance to timely diagnose faults on board to ensure the security and reliability of vessel. There are various types of faults for ships in marine operation, including actuator

faults, sensor faults, and parametric faults. This paper mainly focuses on actuator faults, i.e, to detect thruster failure in DP operation.

Fault diagnosis commonly includes fault detection, fault isolation, and fault estimation, among which, the first two tasks are considered to be mostly important [5]. Methods for fault detection and isolation (FDI) are generally classified into model-based and data-based methods [6].

Model-based approaches that rely on the dynamic model of a system have been widely researched and applied in the past decades. Generally, the faults are modelled as parameter changes, and diagnosis can be performed by state or parameter estimation of the considered system. In [7], thruster fault detection is obtained by a combination of parity space approach and Luenberger observer in an over-actuated offshore supply vessel. In [8], a robust fault detection observer and a time-varying detection criterion are presented to detect the actuator faults distinguished from uncertainties in nonlinear dynamics and external disturbances for underactuated surface vessels. A Gaussian particle filter based diagnosis method was proposed in [9] for autonomous underwater vehicles (AUV). Lin et al. [10] constructed an iterative learning observer to estimate the unknown thruster faults for dynamic positioning of ships, which requires less on-line computing power than adaptive observers. For the model-based detection techniques, an accurate mathematical model of the system is a prerequisite. However, it is not easy to obtain the model due to the varying environmental conditions and the complexity of the system itself.

Compared to data-based methods, the approaches based on historical data do not need a mathematical model, neither much prior knowledge about the system. These characteristics promote an advantage for complex and nonlinear systems, where an explicit model is hard to be obtained. The statistical analysis methods such as principal component analysis [11] [12] are successfully applied to diagnose actuator faults. In addition, machine learning as well as deep learning are also powerful tools to handle the data in fault diagnosing process [13]. A novel convolutional neural network was applied on the fault diagnosis, which demonstrates a significant improvement of prediction accuracy compared with traditional methods [14]. Li et al. [15] proposed a strategy based on a dynamically driven recurrent neural network to detect and isolate thruster

failures in the satellite's attitude control system. In [16], the author presents an approach to fault diagnosis with online detection of novel faults and automatic learning using fuzzy clustering techniques. The method is proved feasible and efficient for actuator fault diagnosis. Kemp et al. [17] developed an unsupervised fault detector based on the performance data of an AUV and verified the detector is efficient in reducing the false alarm rate. The data-based methods work well in fault diagnosis. However, they strongly rely on a large volume of historical data to extract features and establish the fault mode, which is always limited in reality.

Despite the numerous researches on fault detection and isolation, there are still some challenges in DP thruster failure diagnosis. The main challenge is the difficulty of obtaining a realistic model representing ship behavior when interacting with the environment. The environmental disturbances caused by ocean currents, winds and waves have a significant but unpredictable effect on system performance. From research point, the wind interference on DP operation will be firstly taken into consideration in this paper. Based on the DP ship model under wind disturbance, an effective thruster failure detection and isolation scheme is proposed and verified.

The rest of the paper is organized as follows. The following section II presents the proposed model-based fault detection and isolation method framework. DP operation simulation is conducted in Section III to validate the efficiency of the proposed method. Conclusion and future work are shown in Section IV.

## II. FRAMEWORK OF MODEL-BASED FAILURE DETECTION AND ISOLATION METHOD

In this section, an effective failure detection and isolation scheme is proposed for detecting thruster failure in dynamically positioning offshore surface vessels. When one thruster fails to work normally, the ship DP performance will diverge from the fault-free status, thus ship position and orientation in the earth-fixed frame are selected as monitoring state. Failure detection and failure isolation are both included in the proposed framework.

### A. Framework

Fig. 1 gives an overall architecture of the thruster failure detection and isolation scheme. It can be divided into three sections: ship measurements, mathematical modeling, and failure diagnosis. In the real ship experiment or simulator, the DP operation is performed through a DP controller. For a fully actuated offshore surface vessel, the horizontal motions—surge, sway and yaw are of great interest. The control force generated from the controller will be further allocated by an allocation algorithm to corresponding thrusters. And then the vessel can be maneuvered towards the reference point by these thrusters. The simulation process is marked with a red dash line in Fig. 1.

The mathematical model for ship maneuvering in the framework can be derived from through Newton-Euler or Lagrange methods. The interaction between ship hull, propulsion force

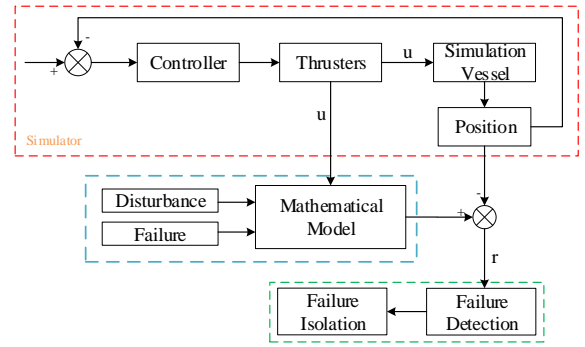


Fig. 1. Thruster failure detection and isolation architecture

and hydrodynamic effect is represented by a set of complex differential equations. At present, there are several variants for ship maneuvering, such as Nomoto model and nonlinear maneuvering model [18].

The residual signal which reflects the variation between model-predicted state and sensor data flows into the fault diagnosis module in the framework. The fault diagnosis module includes two components. The first one is used for detecting the existence of failures; the other one is to isolate the sources of failures. In a predefined detection time window, by applying the thruster command from the controller to the established mathematical model, an estimated ship state will be obtained. A ship behavior-based residual generator in the detection time window is introduced. It is designed to keep low level in fault-free phase, and increase to exceed a threshold when a thruster failure occurs. In the isolation phase, residuals are further analyzed to configure the location of the failure by means of probability analysis. It ends up with a probabilistic model, from which better knowledge about the confidence of failure location, as well as more meaningful information to the end-user, can be gained.

### B. Modeling

For horizontal motion of a fully actuated offshore surface vessel under the wind disturbance, considering the surge, sway and yaw motion components, the linearized motion mathematical model of ship in DP maneuvering is expressed as [19]:

$$\begin{aligned} \dot{\eta} &= J(\eta)\nu \\ M\dot{\nu} + D(\nu)\nu &= \tau + \tau_w \end{aligned} \quad (1)$$

where,  $\eta = (x, y, \psi)'$  is the ship position vector in the earth-fixed frame.  $\nu = (u, v, r)'$  is the ship velocity vector in the body-fixed frame. The rotation matrix is given by

$$J(\eta) = \begin{bmatrix} \cos(\psi) & -\sin(\psi) & 0 \\ \sin(\psi) & \cos(\psi) & 0 \\ 0 & 0 & 1 \end{bmatrix}$$

$M$  and  $D$  are mass and linear damping matrices.  $\tau$  is the generalized control forces which are distributed among the thrusters in terms of control inputs  $\mathbf{u}$ :

$$\tau = T\mathbf{u} \quad (2)$$

where  $\mathbf{u}$  is the thrust force vector. The thruster configuration matrix  $T$  depends on the location and orientation of thrusters.

The wind force acting on the vessel moving at a forward speed are estimated as [19]:

$$\tau_w = \frac{1}{2}\rho_a V_{rw}^2 \begin{bmatrix} C_X(\gamma_{rw})A_{FW} \\ C_Y(\gamma_{rw})A_{LW} \\ C_N(\gamma_{rw})A_{LW}L_{oa} \end{bmatrix} \quad (3)$$

The relative wind speed and attack angle are defined as

$$\begin{aligned} V_{rw} &= \sqrt{u_{rw}^2 + v_{rw}^2} \\ \gamma_{rw} &= -atan2(v_{rw}, u_{rw}) \end{aligned} \quad (4)$$

The relative wind velocities components are  $u_{rw} = u - V_w \cos(\beta_w - \psi)$  and  $v_{rw} = v - V_w \sin(\beta_w - \psi)$ , where  $V_w$  and  $\beta_w$  are the wind speed and its direction respectively.

### C. Fault diagnosis

In DP operation scenario, the vessel is supposed to keep steady at one fixed position  $(x_0, y_0)$  with orientation  $\psi_0$  in the earth-fixed frame. The control force is distributed into each thruster and then the vessel will be propelled towards the fixed point by the corresponding thrust.

In the failure detection module, a detection time window is adopted to evaluate the residuals between model reference sequences and measurement data. The states of the dynamic model under the command thrust can be estimated by solving the model differential equations (1). In the window  $[t_0, t_T]$ , the residuals are defined as

$$r(t) = \sqrt{e_x^2 + e_y^2} \exp(e_\psi) \quad (5)$$

where  $e_x = \hat{x} - x$ ,  $e_y = \hat{y} - y$ ,  $e_\psi = \hat{\psi} - \psi$ ,  $(\hat{x}, \hat{y}, \hat{\psi})$  are estimated ship position and heading,  $(x, y, \psi)$  represents sensor position and heading.

After the residuals are generated, the detection of failure can be performed through the following rules, where  $\delta$  refers to the threshold obtained through several simulation experiments.

$$\begin{cases} r(t) \leq \delta & normal \\ r(t) > \delta & failure \end{cases} \quad (6)$$

Define the initial state of model (1) as  $X(t_0) = [\eta(t_0), \nu(t_0)]$ , with the residual signal  $r(t_0) = 0$ . If there is no residual in the period  $[t_0, t_0 + \Delta t]$  exceeds the threshold, the detected period is judged normal. Then the window slides to the next period  $[t_0 + \Delta t, t_0 + 2\Delta t]$ . This process will continue until abnormal alarm happens. The value of threshold is determined on the basis of larger number of experiments. In this paper, the threshold value is defined as:

$$\delta = \mu + k\sigma \quad (7)$$

where  $\mu$  and  $\sigma$  are the mean and standard deviation of residuals in faulty-free status. The selection of  $k$  value is critical, which represents a trade-off between a low false-alarm rate and a high sensitivity to failures.

Once a fault is detected, the next problem needs to be solved is to distinguish the failure mode. According to the mathematical expression of DP maneuvering, the ship model reference sequences in healthy and different failure conditions can be built respectively. At the time  $t_d$  when fault detection residual surpasses a given threshold, failure isolation can be accomplished by probability analysis between the actual successor sequence and the predicted state sequences based on analytical model. In the detected faulty period  $[t_d, t_e]$ , for each failure mode, a corresponding residual sequence is generated. The mean integral of residual is considered to obtain a quantitative comparison between the results of different failure mode simulations. The mean integral of residual index, normalized with respect to the time length of the faulty period, is expressed as

$$s_i = \frac{1}{T} \int_{t_d}^{t_e} r(t) dt, i = 1, 2, \dots, N \quad (8)$$

where  $N$  represents the number of failure mode. The probability of each failure mode is calculated according to

$$P_i = 1 - \frac{s_i}{\sum_{i=1}^6 s_i} \quad (9)$$

The highest probability indicates that the relevant failure mode has the most similar features with the detected abnormal.

## III. EXPERIMENT

To validate the effectiveness of the proposed thruster failure detection and isolation method, simulation experiments of DP maneuvering under different failure scenarios is conducted.

### A. Experimental setup

All experiments are conducted in a commercial professional simulator developed by Offshore Simulator Centre AS in Norway. It features a simulated environment in which a user may manipulate the wind, waves, and ocean current to mimic real-life conditions. It offers a library of real vessel models to choose from. Fig. 2 shows a view of the simulated environment with the selected vessel engaged in DP operation. Table I provides the vessel's main dimensions.

TABLE I  
DIMENSIONS OF SIMULATION VESSEL

Description	Value
Mass [kg]	$1.0179 \times 10^7$
$L_{pp}$ [m]	82.7
Bredth [m]	23.058
Draught [m]	7.5

The selected simulation vessel is equipped with two main thrusters, two tunnel thrusters at the bow and two tunnel



Fig. 2. Simulation vessel and parameter tuning interface

thrusters at the stern, as shown in Fig. 3. The thruster configuration matrix has the form

$$\mathbf{T} = \begin{bmatrix} 0 & 0 & 0 & 0 & 1 & 1 \\ 1 & 1 & 1 & 1 & 0 & 0 \\ L_1 & L_2 & -L_3 & -L_4 & -L_5 & L_6 \end{bmatrix}$$

where  $L_i (i = 1, \dots, 6)$  are the moment arms in yaw. The allocation of the six thrusters is symmetrical with respect to the longitudinal axis of the vessel. The two main thrusters, two bow tunnel thrusters and two stern tunnel thrusters are considered as three pairs of thrusters, and the same force demand is applied to both thrusters in each pair when they are running in fault-free status. It is worth noting that in the selected vessel, the bow tunnel thrusters and stern tunnel thrusters are located near, where the distance  $d_b$  and  $d_s$  are quite small, almost  $1/40$  of the vessel length.

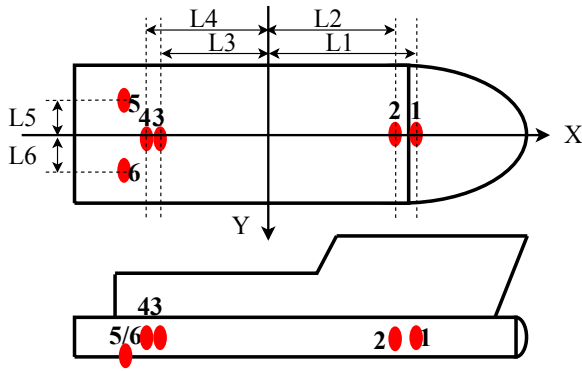


Fig. 3. Thruster configuration for the offshore surface vessel.

For the specific simulation study performed in this paper, constant environmental parameters are applied. The relevant parameters in wind model (3) are presented in Table II.

### B. Simulation results

In order to verify the effectiveness of the proposed method, simulation experiments under different thruster failure modes

TABLE II  
PARAMETERS OF WIND FORCE MODEL

Symbol	Description	Value
$A_{FW}$	Frontal projected area of ship [ $m^2$ ]	470
$A_{LW}$	Lateral projected area of ship [ $m^2$ ]	965
$L_{oa}$	Wind characteristic vessel length [ $m$ ]	93.5
$\rho_a$	Air density [ $kg/m^3$ ]	1.247
$C_X, C_Y, C_N$	Wind coefficients	—

are carried out. Single thruster failure cases are designed as Table III shows, where '0' refers to 100% thruster invalid and '1' represents normal status.

TABLE III  
THRUSTER FAILURE CASES OF SIMULATION

Case	th1	th2	th3	th4	th5	th6
011111	0	1	1	1	1	1
101111	1	0	1	1	1	1
110111	1	1	0	1	1	1
111011	1	1	1	0	1	1
111101	1	1	1	1	0	1
111110	1	1	1	1	1	0

Fig. 4 shows the residual results of two bow tunnel thrusters failure. This failure is characterized by an abrupt invalid of a thruster, whose actual speed freezes at 0 while command speed is as normal. From the residual graph (Fig. 4), it can be seen that the fluctuations of the residual signal at  $t = 531.4s$  and  $t = 1421.4s$  are obviously strong, implying failure happens. If the residual value is greater than the threshold, then it can be judged failure. For a low false alarm rate, the threshold (red dash line) should be set no less than  $k = 1$  for bow tunnel thruster detection. For the two detected faulty periods,

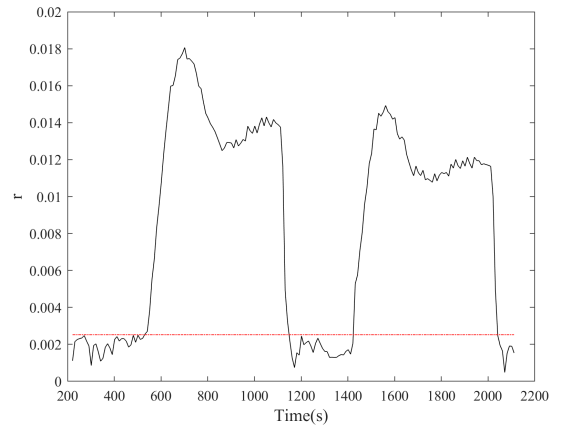


Fig. 4. The residual signal of bow thruster failure mode

to determine the location of the failed thruster, the residual sequence of each failure mode is generated, as shown in Fig. 5(a)-(b). It shows that individual residual result, which

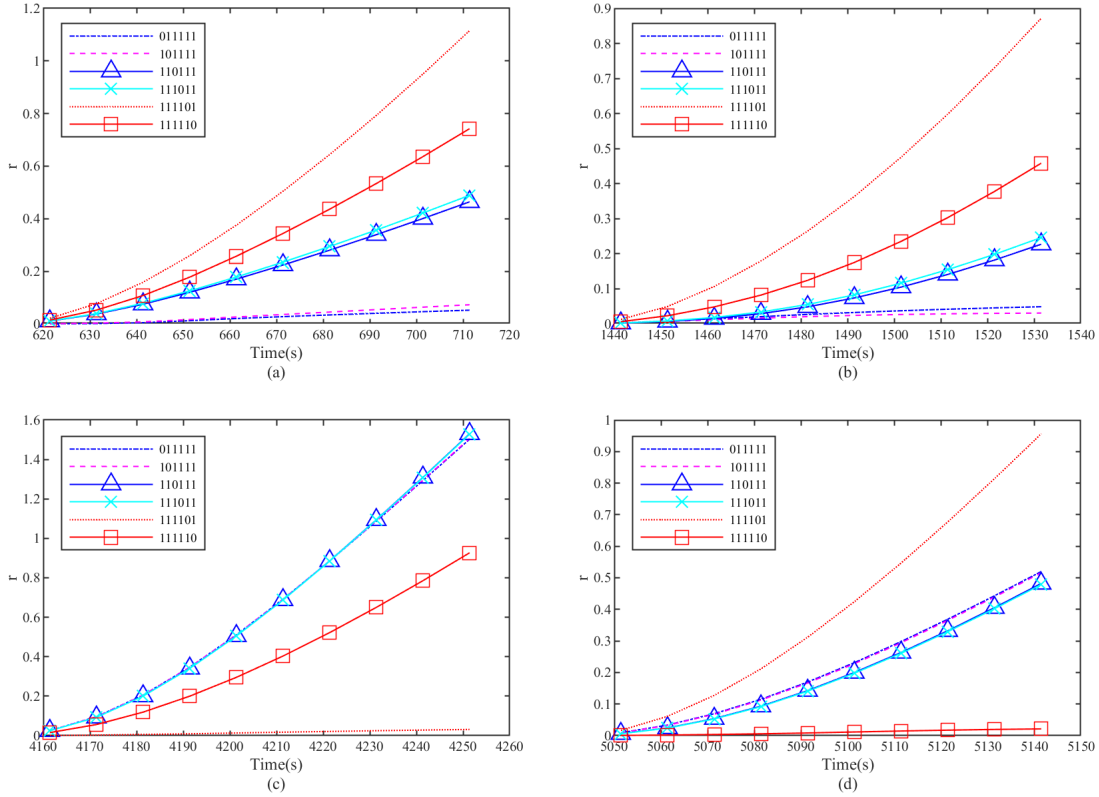


Fig. 5. Residuals of each failure mode in detected faulty period. (a) first anomaly in bow thruster; (b) second anomaly in bow thruster; (c) first anomaly in main thruster; (d) second anomaly in main thruster.

indicates the variation from the measurement data is increasing with time accumulation. Lower residual represents higher consistency between the estimated state and sensor state. From Fig. 5(a)-(b), we can get that in the first abnormal period, the performance of the ship is the most similar to 011111 failure mode, and the second period 101111. The probability of each failure mode is analyzed according to the rule (9) and the results are presented in Fig. 6. It is worth mentioning that in these two faulty cases, 011111 and 101111 failure modes have a pretty high similarity, manifested in little difference in diagnosis probability. The reason is that these two bow thrusters are located quite close to each other. The similar isolation results are also obtained from the comparison of two stern tunnel thrusters, which are also implied in Fig. 6. During tunnel thruster failure isolation, it is not easy to separate one from the other near located, while by using the proposed method, one can clearly isolate the failed pair of thrusters. On the basis of the differentiated pair, the mode with a higher probability is diagnosed as a failure.

Analysis of main thruster failure performance is followed. The residuals caused by each main thruster failure characterize different peak values in Fig. 7. This is caused by the position difference of two main thrusters to the wind direction. Here the threshold for failure detection is also set at  $k = 1$ .

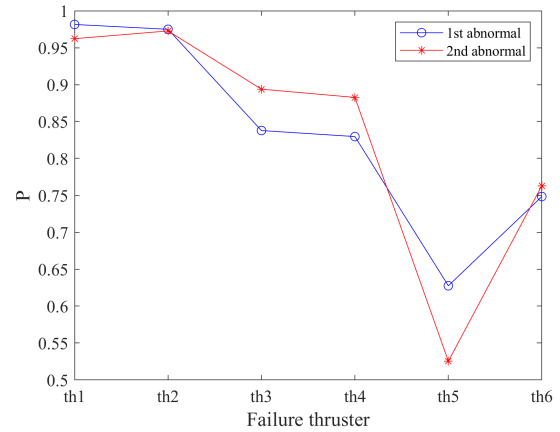


Fig. 6. Probability analysis results of two detected abnormal period.

The failure mode residual comparison results are presented in Fig. 5(c)-(d). It can be seen that the main thruster failure has rather different features compared with tunnel thruster failure due to the fact that main thrusters and tunnel thrusters provide disparate force to maintain the ship's position under wind disturbances. According to Fig. 8, one can get that the first

detected anomaly is caused by port main thruster failure and the second starboard main thruster.

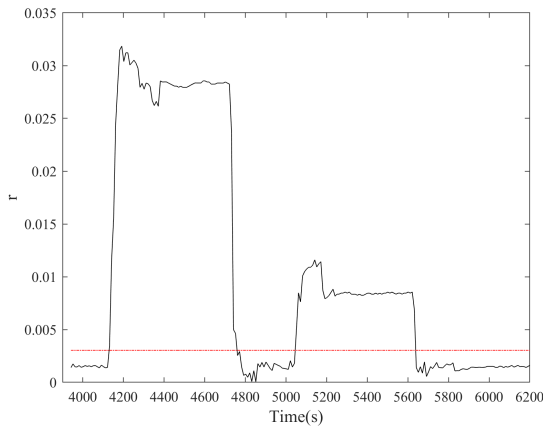


Fig. 7. Residual signal of main thruster failure cases.

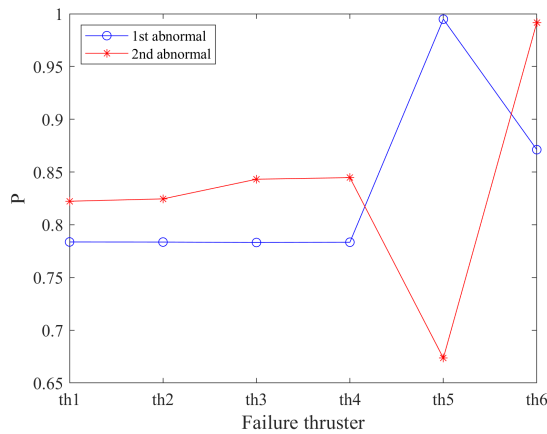


Fig. 8. Probability analysis results of two detected abnormal period.

#### IV. CONCLUSION

In this paper, an effective model-based thruster failure detection and isolation method for a dynamically positioned offshore surface vessel has been proposed. A general thruster failure detection and isolation scheme and a new attitude-based residual generator for DP vessels have been given. By introducing the probability analysis, the failure isolation can be completed through probability comparison. The effectiveness of the proposed approach has been verified through the comparison simulation results on a typical offshore surface vessel. In future work, a further investigation of failure separation between two close thrusters will be conducted, as well as more complex environmental disturbances.

#### ACKNOWLEDGMENT

This work was supported by the MAROFF KPN project “Digital Twins for Vessel Life Cycle Service” (Project no.: 280703). The authors would like to thank the technical support from Offshore Simulator Centre AS.

#### REFERENCES

- [1] J. Lee, M. Ghaffari, and S. Elmeligy, “Self-maintenance and engineering immune systems: Towards smarter machines and manufacturing systems,” *Annual Reviews in Control*, vol. 35, no. 1, pp. 111–122, 2011.
- [2] R. Beckwith *et al.*, “Managing big data: Cloud computing and co-location centers,” *Journal of Petroleum Technology*, vol. 63, no. 10, pp. 42–45, 2011.
- [3] A. J. Sørensen, “A survey of dynamic positioning control systems,” *Annual Reviews in Control*, vol. 35, no. 1, pp. 123–136, 2011. [Online]. Available: <http://www.sciencedirect.com/science/article/pii/S1367578811000095>
- [4] T. A. Johansen, T. I. Bø, E. Mathiesen, A. Veksler, and A. J. Sørensen, “Dynamic positioning system as dynamic energy storage on diesel-electric ships,” *IEEE Transactions on Power Systems*, vol. 29, no. 6, pp. 3086–3091, Nov 2014.
- [5] C. Gao, Q. Zhao, and G. Duan, “Robust actuator fault diagnosis scheme for satellite attitude control systems,” *Journal of the Franklin Institute*, vol. 350, no. 9, pp. 2560 – 2580, 2013. [Online]. Available: <http://www.sciencedirect.com/science/article/pii/S0016003213000914>
- [6] P. M. Frank, “Fault diagnosis in dynamic systems using analytical and knowledge-based redundancy: A survey and some new results,” *Automatica*, vol. 26, no. 3, pp. 459 – 474, 1990. [Online]. Available: <http://www.sciencedirect.com/science/article/pii/000510989090018D>
- [7] F. Benetazzo, G. Ippoliti, S. Longhi, and P. Raspa, “Advanced control for fault-tolerant dynamic positioning of an offshore supply vessel,” *Ocean Engineering*, vol. 106, pp. 472 – 484, 2015. [Online]. Available: <http://www.sciencedirect.com/science/article/pii/S0029801815003054>
- [8] B. S. Park and S. J. Yoo, “Fault detection and accommodation of saturated actuators for underactuated surface vessels in the presence of nonlinear uncertainties,” *Nonlinear Dynamics*, vol. 85, no. 2, pp. 1067–1077, Jul 2016. [Online]. Available: <https://doi.org/10.1007/s11071-016-2744-y>
- [9] Y. S. Sun, X. R. Ran, Y. M. Li, G. C. Zhang, and Y. H. Zhang, “Thruster fault diagnosis method based on Gaussian particle filter for autonomous underwater vehicles,” *International Journal of Naval Architecture and Ocean Engineering*, vol. 8, no. 3, pp. 243–251, 2016. [Online]. Available: <http://dx.doi.org/10.1016/j.ijnaoe.2016.03.003>
- [10] Y. Lin and J. Du, “Fault-tolerant control for dynamic positioning of ships based on an iterative learning observer,” in *2016 35th Chinese Control Conference (CCC)*, July 2016, pp. 1116–1122.
- [11] Y. Jiang, B. He, P. Lv, J. Guo, J. Wan, C. Feng, and F. Yu, “Actuator Fault Diagnosis in Autonomous Underwater Vehicle Based on Principal Component Analysis,” *2019 IEEE International Underwater Technology Symposium, UT 2019 - Proceedings*, 2019.
- [12] T. Ait Izem, W. Bougheloum, M. F. Harkat, and M. Djeghaba, “Fault detection and isolation using interval principal component analysis methods,” *IFAC-PapersOnLine*, vol. 28, no. 21, pp. 1402–1407, 2015. [Online]. Available: <http://dx.doi.org/10.1016/j.ifacol.2015.09.721>
- [13] A. L. Ellefsen, V. Æsøy, S. Ushakov, and H. Zhang, “A comprehensive survey of prognostics and health management based on deep learning for autonomous ships,” *IEEE Transactions on Reliability*, vol. 68, no. 2, pp. 720–740, June 2019.
- [14] L. Wen, X. Li, L. Gao, and Y. Zhang, “A new convolutional neural network-based data-driven fault diagnosis method,” *IEEE Transactions on Industrial Electronics*, vol. 65, no. 7, pp. 5990–5998, July 2018.
- [15] L. Li, L. Ma, and K. Khorasani, “A dynamic recurrent neural network fault diagnosis and isolation architecture for satellite’s actuator/thruster failures,” in *Advances in Neural Networks – ISNN 2005*, J. Wang, X.-F. Liao, and Z. Yi, Eds. Berlin, Heidelberg: Springer Berlin Heidelberg, 2005, pp. 574–583.
- [16] A. Rodríguez-Ramos, A. J. da Silva Neto, and O. Llanes-Santiago, “An approach to fault diagnosis with online detection of novel faults using fuzzy clustering tools,” *Expert Systems with Applications*, vol. 113, pp. 200–212, 2018.
- [17] M. Kemp and B. Raanan, “Actuator Fault-Detection for Autonomous Underwater Vehicles Using Unsupervised Learning,” *Annual Conference of the Prognostics and Health Management Society 2017*, p. 7, 2018.
- [18] R. Skjetne, Ø. Smogeli, and T. I. Fossen, “Modeling, identification, and adaptive maneuvering of CyberShip II: A complete design with experiments,” pp. 65–70, 2004.
- [19] T. Fossen, *Handbook of Marine Craft Hydrodynamics and Motion Control*. John Wiley & Sons, 2011.